Int. J. Electrochem. Sci., 10 **(2015)** 9907 - 9918

International Journal of ELECTROCHEMICAL SCIENCE
www.electrochemsci.org

Short Communicatin

Synthesis, Photo Physical Studies and Evaluation of Ruthenium(II) Complexes of Polypyridyl Ligands as Sensitizer for DSSCs

Andile C. Mkhohlakali, Peter A. Ajibade[*]

Department of chemistry , Faculty of Science and Agriculture, University of Fort Hare, Private Bag X 1314, Alice 5700, South Africa**.**
[*]E-mail: pajibade@ufh.ac.za

Received: 9 August 2015 / *Accepted:* 30 September 2015 / *Published:* 4 November 2015

In the research on TiO_2 nanocrystalline sensitization, ruthenium(II) complexes have received considerable attention in order to get efficient dyes for DSSCs. In this study, we report the synthesis of ruthenium(II) complexes formulated as $[Ru(L_1)(L_2)(NCS)_2]$, $[Ru(L_3)(L_1)((NCS)_2]$ where L_1= 1,10-phenanthroline-4,7-disulphonic acid, L_2= 2,2'-bipyridine-4,4'-dicarboxylic acid and L_3 = 1,10-phenanthroline-2,9-dicarboxy aldehyde. The compounds were characterized by ^{1}H-NMR, FTIR, UV-Vis and fluorescence spectroscopy. The complexes exhibited a broad metal-to-ligand charge transfer (MLCT) absorption bands in the range 510-531 nm and intense (π-π*) transitions between 240-380 nm. Some of these complexes showed emission maxima up to 680 nm. The compounds were used sensitizers to fabricate solar cells and an overall conversion efficiencies of 0.2-1.06 % under standard 1 sun 1.5 AM illumination (100 $mWcm^{-2}$) with open circuit voltage 0.53, and 0.6, 0.48 V, short circuit current density up to 3.4 $mAcm^{-2}$ and fill factor up to 0.6 were obtained.

Keywords: DSSCS; Ruthenium(II) polypyridyl complexes; short circuit current voltage; open voltage solar cell efficiency,; photo physical properties.

1. INTRODUCTION

Dye sensitized solar cells (DSSCs) are based on sensitization of TiO_2 semiconductor [1], electrolyte and the dyes as sensitizers. DSSCs technology because of its low cost, and relatively high performance, has attracted many researchers in the field of photovoltaic technology as promising alternative to conventional silicon based solar cell [2] and to replace nonrenewable fossil fuels. The main component for dye sensitized solar cell is the dye-sensitizer [2,3], of which in this work is ruthenium polypyridyl metal complexes. Metal complexes based on 1,10-phenanthroline and

bipyridine has been used extensively for dye-sensitized solar cell, fluorescence probe and other applications [5]. The photophysical and electrochemical properties of prototype $[Ru(bpy)_3]^{2+}$ received considerable attention on ruthenium polypyridyl complexes about 30 years ago [4,6]. This follows the pioneering work of Gratzel on ruthenium(II) poypyridyl based dye-sensitized solar cells in 1991 [2, 7]. The archetype ruthenium(II) complexes in this field was N3, N719 as sensitizer for TiO_2 sensitization, that gave about 7-10 % solar-to- energy conversion efficiencies [8]. The study dates back to the history of photosensitization of wide band gap semiconductors [9] adopted from convergence of photography in the 19^{th} century [10-11].

In this work, we report the synthesis of ruthenium(II)complexes of phenanthroline functionalized with sulphonic acid and aldehyde moieties mixed 4,4'-dicarboxylic acid-2,2'-bipyridine. The compounds were characterized with FTIR, UV-Vis, photoluminescence and NMR spectroscopic techniques. The ruthenium compounds were used to fabricate solar cells and their performance on TiO_2 nanoctrystalline was examined using photocurrent-voltage (J-V) curves.

2. EXPERIMENTAL

2.1 Materials

All chemicals were purchased from Sigma-Aldrich, and were used as obtained. 1,10-phenanthroline-4,7dichloro was sulfonated using excess sodium disulfate (Na_2SO_3) as described in the literature [12]. Iodide redox electrolyte (solaronix), fluorine doped tin oxide ($F:SnO_2$) substrate, colloidal TiO_2 (solaronix), scotchtape (solaronix) copper conductive tape, soldering iron, surlyn film (solaronix) were used as obtained.

2.2 Synthesis of 1,10-phenanthroline-4,7-disulphonic acid (L1)

In 100 mL 2 neck flask, 1,10-phenanthroline-4,7-dichloro (100 mg, 0.44 mmole), sodium sulphate (0.566, 10 eqv) excess was added to ethanol: water (1:1v/v) (18 mL), the reaction mixture was refluxed at 80 °C for 72 hours. Then the reaction was allowed to cool to room temperature and the solvent was reduced *in vacuum*. The white precipitate formed was collected using a G4 crucible sintered glass, and the product was washed using distilled water.

Yield = 1.1126 g, 76 %, Mp = >300 ^oC, IR (cm^{-1}): 3329, 1675, 1210, 848, 759, 617. (^1H NMR, DMSO-d6) σ (ppm): 8.87; 8.86; 8.321; 7.86; 7.84.

2.3 Synthesis of 1,10-phenanthroline-4,7-dicarboxyaldehyde

In 100 mL two neck flask, 1,10-phenanthroline-2,9-dimethyl (neucuproine) (0.028 g, 0.29 mmole) was added, and selenium dioxide in 1.4 dioxane: distilled water (95:5 %) (45:2.5 mL) was prepared separately and it was added directly into the flask, the reaction was stirred for 5-10 min, and refluxed at 100 °C for 4 hours. The solution was poured while it is hot using a G4 crucible sintered

glass, and the black solid remains were collected on sintered glass, the yellow filtrate was taken to rotatory evaporator to remove the solvent and the yellow residue formed was collected and precipitated using diethyl ether. Pale yellow product was obtained and washed with diethyl ether.

Yield = 0.92 g, 52 %, MP (>300 °C) = 158; IR (cm^{-1}) = 1726, 2012, 2953, 3512, 3550. (^{1}H NMR DMSO-d6): σ(ppm) 8.31; 8.324, 8.416, 8.877; 8.79; 8.80; 9.964.

2.4 Synthesis of 2.2'-bipyridine-4.4'-ducarboxylic acid

4,4'-dimethyl-2.2'-bipyridine (1000 mg; 5.43 mmol) was dissolve in 30 mL of sulphuric acid at room temperature, and to this solution, sodium dichromate (6100 mg; 23 mmol) was added in portion for 4 hours, to oxidize methyl groups to carboxylate group. The reaction flask was heated to 80 °C for 12 hours while stirring. The reaction was cooled, and thereafter was poured into ice water (200 mL) and kept at 0 °C for 12 hours. The formed suspension was filtered by suction. The expected green-yellow precipitate separated was washed with distilled water till it turned colourless. The solid was suspended in concentrated nitric acid and refluxed for 8 h, and then poured to an ice water for 12 h to give a white powder.

Yield = 0.12 g, 89 %, Mp: 295 °C, IR (nujol, cm^{-1}): 3415; 3548; 1620; 1721; 1292; 1367. ^{1}H NMR (DMSO-d_6): 8.88; 8.86; 8.87; 8.72; 8.73; 8.09; 8.08.

2.5 Synthesis of ruthenium(II) polypyridyl complexes

All ruthenium(II) polypyridyl complexes were synthesized using tetrakis(dimethyl sulfoxide) dichloro ruthenium, $[Ru(dmso)_4Cl_2]$ which was synthesized following literature procedure [13, 15] and used as precursor material to synthesize the complexes as reported in the literature [16].

2.6 Synthesis of Ru-1

In 100 mL two neck flask, $[Ru(dmso)_4Cl_2]$ (100 mg, 0,22 mmole) was dissolved in N,N dimethyl formamide (30 mL) and the solution was stirred at room temperature for 5-10 min, then 1.0-phenanthroline-4,7-disulphonic acid (136 mg, 0.44 mmole) was added and the reaction refluxed at 80-100 °C under nitrogen gas for 5 hours during which time the reaction was covered with aluminum foil to reduce the light. To this deep brown solution, 4.4'-dicarboxylic acid-2.2'-bipyridine (107 mg, 0.44 mmole) was added and the reaction was heated to reflux at 120-140 °C in the dark for about 4 hour, and then excess potassium thiocyanate (500 mg) was added as solid to this solution, and the temperature was raised to 150 °C to reflux for another 4 hours after which the solution turned to reddish-brown. The solvent was reduced in vacuum and acetone was added to precipitate the product was filtered, washed with acetone: ether and shiny dark solid was obtained. Yield = 1.02 g, 60 %, Mp = 234 °C, IR (nujol υ(cm^{-1}): 3729; 2920.28; 2856; 2096; 1670.23; 1254,.UV-Vis (λ_{max}, nm): 305; 366; 533.

2.7 Synthesis of complex Ru-2

In 100 mL two neck flask $[Ru(dmso)_4Cl_2]$ (0.22 mmole), L_1 (0.44 mmole) was dissolved in DMF (45 mL), the mixture was stirred for 5-10 min, and then refluxed at 80-100 ^oC under nitrogen gas for 4 h, the reaction flask was covered with aluminum foil to reduce the light. Subsequently, L_2 (0.44 mmole) was added and the temperatures adjusted to 120 °C and refluxed for 4 h maintain the dark conditions. Finally an excess potassium thiocyanate was added and refluxed to 140 °C for another 4 h and the solvent was then reduced in vacuum.

Acetone was used to precipitate the reddish-brown product that was obtained. Yield = 0.986 g, 58 %, Mp = > 300 °C colour = reddish-brown, IR (nujole, cm^{-1}): 3385, 2920; 2093; 1646.69; 1376; 1456; 1238.52; 1067; 759. Uv-Vis (λ_{max} nm): 300; 380; 531.

2.8 Synthesis of Ru-3

In 100 mL two neck round bottom flask, $[Ru(dmso)_4Cl_2]$ (0.2 mmole) was dissolved in DMF (30 mL) and the reaction was stirred for 5-10 min, then 2,2'-bipyridine (4.119 mmole) was added and the reaction was purged with nitrogen and heated to reflux at 80-100 °C for 4 h. The solution turn to purple brown, subsequently L_2 (0.4199 mmole) was added and the heating was adjusted to reflux the solution at 120-140 °C for 4 h, to this solution an excess of potassium thiocyanate was added and the reaction was refluxed at 150 °C for another 4 h. The solvent was removed completely using rotatory evaporator and the crude product was dissolved in dichloromethane. The solvent was reduced in vacuum and n-hexane was used to precipitate the reddish-brown solid was collected using crucible sintered glass, and filtered by suction. Yield =1.05 g, 77 %, Mp = >300 °C, IR (nujole, cm^{-1}):3175.73; 2107.18; 1619.03; 1461.05; 1376.43; 847.97; 617.69; 377.05. UV-Vis ($\lambda_{max,}$ nm): 278, 346, 523.

2.9 Solar cell fabrication and characterization

This solar cells were fabricated by adopting reported literature methods [17-20] with slight modifications. The fluorine doped tin oxide (F: SnO2) substrate was used throughout the fabrication process of the dye-sensitized solar cells. The glasses were carefully cuts into area of 0.6 cm^{-2} and were washed with paraffin, followed by isopropanol ad then acetone, because cleaning is the crucial factor for homogeneity and adherence for future coating. After air dry, doctor blading technique with colloidal TiO_2 paste using glass rod for coating the glass substrate, was applied. The coated glass was sintered at 450 °C for 4 h using furnace. The thin film was immersed into $2x10^{-4}$ M solution of ruthenium complex at 60 °C for 8 hours. The soldering iron was used to heat up surlyn film for two electrodes to be glued during sandwiched of the two glass electrodes and then clamped. Finally, iodine electrolyte was injected through the drilled holes using syringe and those holes were covered with tape.

3. RESULTS AND DISCUSSION

3.1 Infrared spectra studies

The FT-IR spectrum of the complex $[Ru(dsphen)(dcbpy)(NCS)_2]$ show similar stretching frequency as that of the ligand, but there is a unique broad, intense absorption band at 2101 cm^{-1} which

is due to υ(CN) vibrational stretching mode of thiocyanate, bonded to the metal center. This band is three to four times more intense compared to band exhibited at 810 cm^{-1}, which is due to υ(CS) of thiocyanate. The band at 807 cm^{-1} show the υ(CS) of sulphonic group bonded to 1,10-phenathroline, this spectrum also shows the absence of υ(C-Cl) band from the starting material (1,10-phenanthroline-4,7-dichoro). The peak at around 848 cm^{-1} is due to υ(S=O) of sulfonic acid and the peak around 1238 cm^{-1} is assigned to the υ(CS-O) stretching vibrations [21]. The spectrum of the complex, $[Ru(dcalphen)(dcbpy)(NCS)_2]$ shows a unique and prominent peak at 2101 cm^{-1}, this peak is assigned to υ(-NCS) stretching vibration the thiocyanate group and confirms the N-coordination to the metal center. There is also another confirmation of the thiocyanate group N-coordination to metal center at 802 cm^{-1} ascribed to υ(CS) vibration band, because NCS^- has two characteristic modes [21]. This peak is four times less intense compared to that of N-coordination [15]. The intense signal at 1671 cm^{-1} can be assigned to υ(C=O) stretching vibration of the carbonyl group of the carboxylic acid. There is also υ(C-O) stretching vibration at 1375 cm^{-1} and 1306 cm^{-1} due to υ(C-O) of aldehyde and carboxylic acid respectively. The absorption peaks at 2857-3366 cm^{-1} corresponds to stretching vibration of υ(C-H) of aromatic ring of polypyridyl ligands and O-H of the carboxylic acid. The FTIR spectrum of $[Ru(bpy)(dcbpy)(NCS)_2]$ complex, shows absorption at 2923-3369 cm^{-1} which can be assigned to the aromatic υ(C-H) stretching band of bipyridine ligand and the hydroxyl group of carboxylic acid at 4,4'-position of bipyridine. The peak at 2089 cm^{-1} can be attributed to υ(NCS) and the peak at 726 cm^{-1} is assigned to υ(CS) stretching vibration.

3.2 ^{1}HNMR spectra of the ligands

The ^{1}H NMR spectrum of 1,10-phenanthroline-4.7-disulfonic acid (L_1) is shown in Figure 1. A prominent peak showed a doublets at 8.87 and 8.86 ppm, this is due to protons at 2,9-positions of 1,10-phenanthroline (d, 2H), which are deshielded due to electron rich carbon that is adjacent to nitrogen of 1,10-phenanthroline. There is also a peak that appeared as a doublet at 8.32 ppm which could be assigned to protons at 3,8-positions, this could be ascribed to it being adjacent to the carbon that is bonded to electron rich sulfur at 4,7-positions. The doublets (d, 2H) appeared up-field in the spectrum could be assigned to protons at 5,6 positions of the phenanthroline ring. In the case of L2, the ^{1}H NMR is shown in Figure 2, and showed three doublets at 3,3'; 5,5' and 6,6' positions of the bipyridine moiety. The resonance at 8.88 ppm and 8.87 ppm can be assigned to the proton at 6.6'-ortho position to the nitrogen of bipyridine which is downfield and deshielded by the attached electronegative nitrogen atom (d, 2H). There is a doublet (d, 2H) at 8.73, 8.72 ppm which is assigned to proton at 3,3' and is downfield which could be the results of being ortho to electron rich carboxyl group. This spectrum also show another resonance with doublet (d, 2H) up field that can be assigned to proton at 5, 5' position of bipyridine.

In Figure 3, the ^{1}H NMR spectrum of L_3 shows a resonance at σ 8.80 ppm which could be assigned to the proton at the para position with high electronegative nitrogen of the 1,10-phenanthroline which is doublet (2d, 2H) at 4,7-position. The prominent peak (2d, 2H) of the aldehyde was observed downfield at 9.96 ppm, and the proton was deshielded downfield by the

electron rich carboxyl group. There is also a resonance at around 8.79 ppm and 8.80 ppm which could be assigned to (d, 2H) to the proton at 3,8 position of 1,10-phenathroline. There is also a doublet which could be assigned to protons at 5,6 position on the phenanthroline ring.

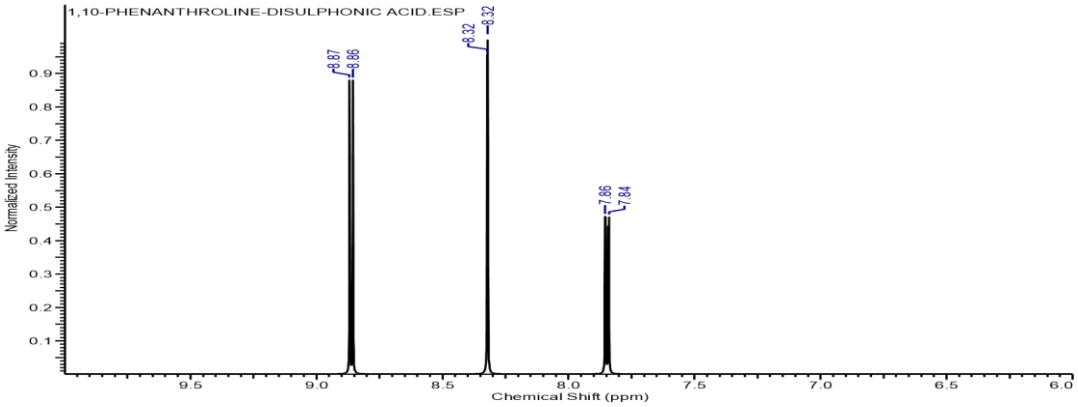

Figure 1. ^{1}H NMR spectrum of ligand1 (L1**)** (dsphen) in $(CD_3)_2SO$

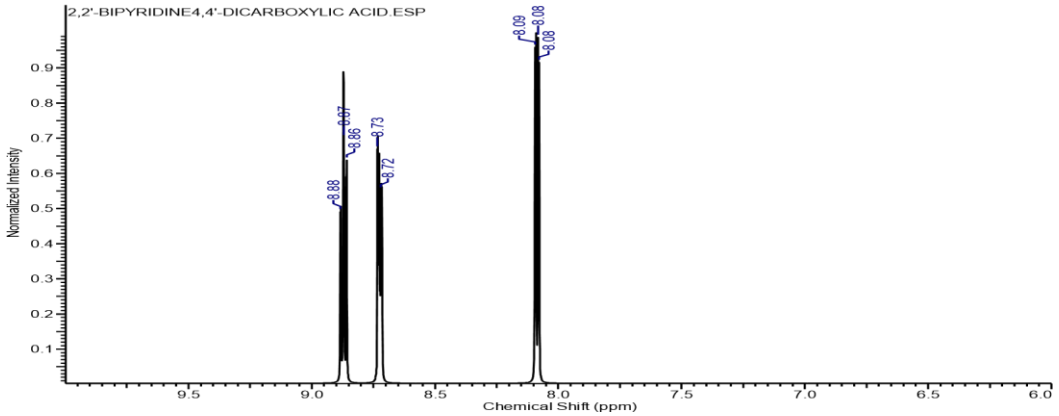

Figure 2. ^{1}H NMR spectrum for L_2 (dcbpy) in $(CD_3)_2SO$

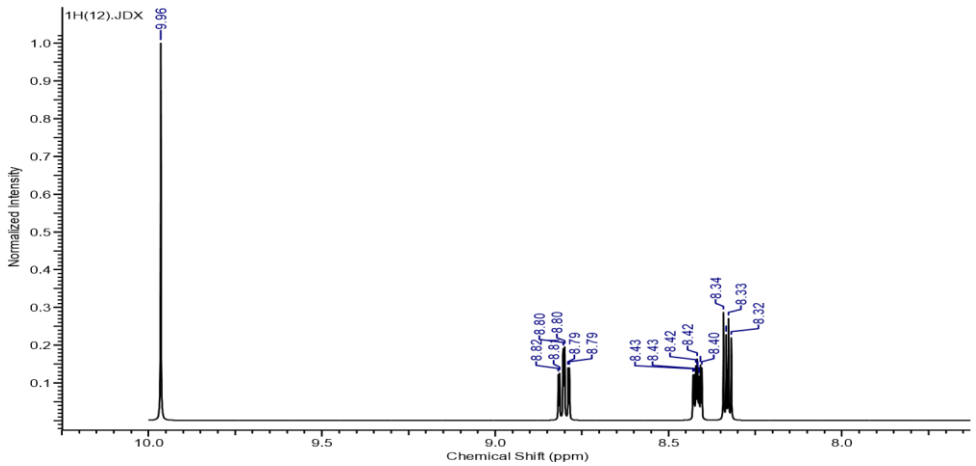

Figure 3. ^{1}H NMR spectrum of L3 (dcaldphen) in $(CD_3)_2SO$

3.3 Electronic spectra of ruthenium(II) polypyridyl complexes

The absorption spectra of three different ruthenium complexes (Ru-1, Ru-2 and Ru-3) in different solvents depending on their solubility, are shown in Figure 4. The absorption spectra of these ruthenium(II) polypyridyl complexes showed two well distinct shoulder band (π-π*) at 316-396 nm which ascribed to intraligand and metal to ligand charge transfer transitions at ultraviolet region. In the visible region, prominent d-d transitions were observed in the range 510-533 nm that could be ascribed to Ru(II) in octahedral environment.

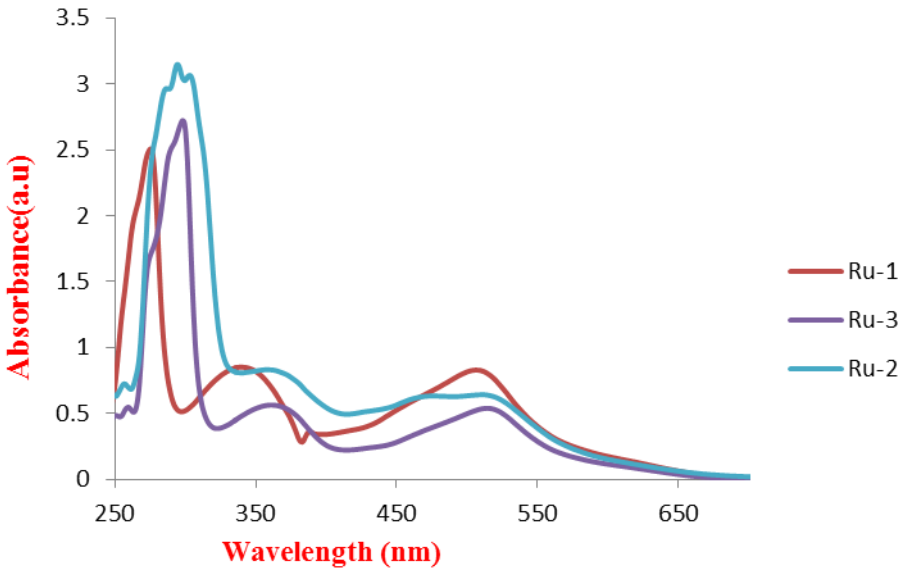

Figure 4. Electronic spectra of the ruthenium(II) polypyridyl complexes

The electronic spectra of the ruthenium complexes: Ru-1, [Ru(daldphen)(dcbpy)$(NCS)_2$]; Ru-3, [Ru(dcbpy)(bpy)$(NSC)_2$] and Ru-2, [Ru(dsphen)(dcbpy)$(NCS)_2$] showed strong and intense absorption bands around 281 nm, 310 nm and 301 nm respectively. These bands are attributed to intraligand (π-π*) transitions within the polypyridyl ligands. The broad bands at 532, 511 and 524 nm respectively are ascribed to the d-d transitions that are peculiar to the absorption properties of ruthenium(II) polypyridyl complexes [22]. These could make the complexes promising candidates for photosensitization for dye-sensitized solar cells, because they absorb the light in the visible region of the electromagnetic spectrum. The (MLCT) band of Ru-1 red shifted with 11 nm compared to Ru-3 is probably due to substitution on the 1,10-phenanthroline at 2,9-position more than ordinary bipyridyine. Ru-1 also have a MLCT bathochromic shift of 2-4 nm compared to that MLCT of Ru-2, this is probably due to the fact that dicaboxaldhyde substituent on phenanthroline have low lying π*- orbital level than the one with sulphonic acid at the peripheral positions. That could enhance absorption of MLCT band to a bit higher region because the energy gap between Ru_{t2g} and π* ligand orbitals is reduced and electron sufficiently transferred from dπRu to π*-orbital of a ligand.

3.4 Emission of ruthenium(II) polypyridyl complexes

In the ruthenium complexes: Ru-1, Ru-2 and R-3 upon their excitation from singlet ground state (^{1}MLCT $_{EXC}$=532 nm) to the triplet excited state ^{3}MLCT, the complex exhibited maxima at 702 nm, 696 nm at room temperature. The carboxaldehyde (COH) group lowered LUMO than sulfonic group (SO_3H) which is centered on the ligands and hence influenced better emission wavelength. The HOMO which centered on the common Ru-NCS, NCS disturbed the t_2g of Ru metal center. The higher intensity of Ru-1 than Ru-2 may suggest the longer excitation lifetime, because higher molecular coefficient is expected, it is therefore expected to be a better sensitizer for dye-sensitized solar cell.

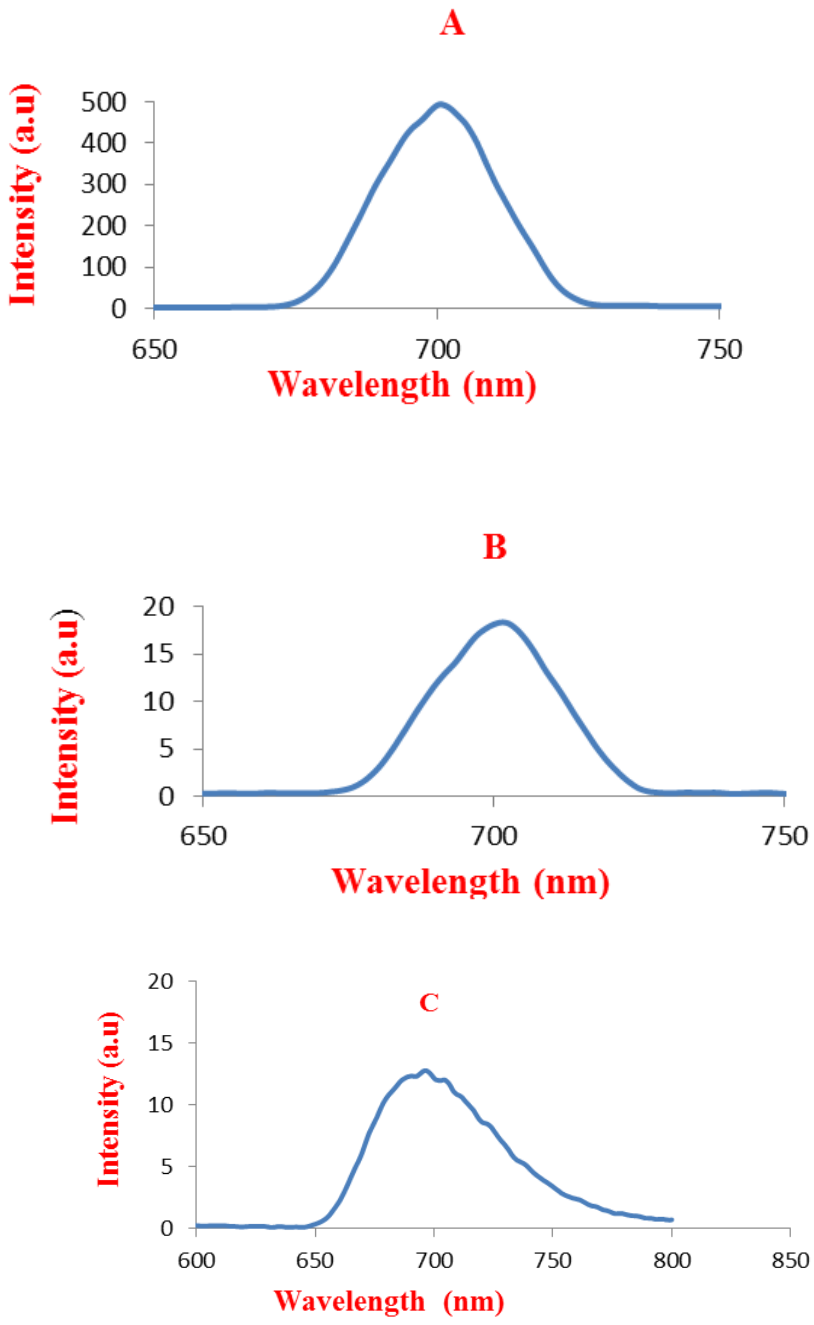

Figure 5. Electronic spectra of the complexes [Ru(dsphen)(dcbpy)(NCS)$_2$] (A), [Ru(dcald)(dcbpy)(NCS)$_2$] (B) and [Ru(bpy)(dcbpy)(NCS)$_2$] in DMF

3.5 Photoelectrochemical measurements

The solar cell efficiency for each ruthenium complex was calculated from the key parameter obtained from I-V curve characterization using equation 1.

$$\eta(\%) = \frac{J_{SC} \times V_{OC} \times FF}{P_{in}} \times 100(\%) \quad \text{.....(1)}$$

Where J_{SC} is short circuit current density, V_{OC} is the open circuit voltage, FF is the fill factor, P_{in} is the incident light at 100mWcm^{-2} [19, 24, 25]. DSSCs efficiency were collected using two electrode set up, with (i) FTO/Pt catalyst as counter electrode and the (ii) FTO/TiO_2/ruthenium(II) polypyridyl complex dye as working electrode. The (J-V) curves are presented in Figure 6 for the dye-sensitized solar cells and more details about the different parameters are listed in Table 1. The photovoltaic performance is measured under 1 sun 1.5 AM illumination at 100 mWcm^{-2}. Ru-1 sensitized solar cell presented a short circuit photo current (J_{SC}) 0.78 mAcm^{-2}, an open circuit voltage (V_{OC}) 0.53 V and fill factor (FF) 0.51 and render an overall conversion efficiency (η) 0.211 %. Under the same conditions Ru-2 sensitized solar cell gives a value (J_{SC}) 2.789 mAcm^{-2}, a (V_{OC}) 0.593 V, and (FF) 0.498 V and exhibited an overall conversion efficiency (η) 0.82 %.

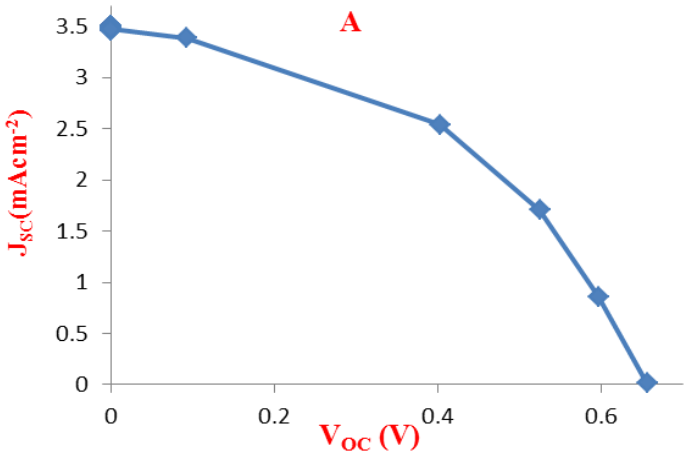

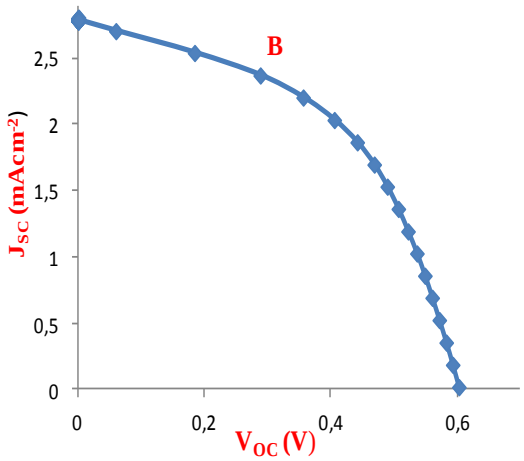

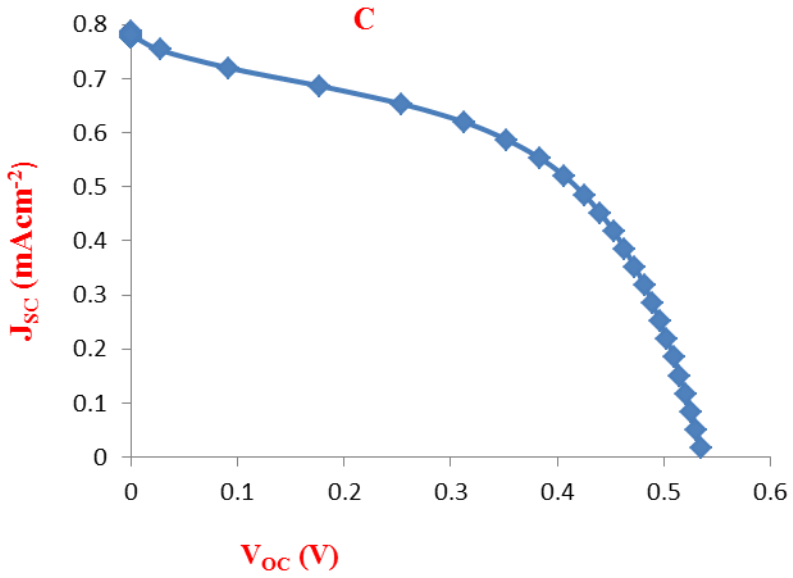

Figure 6. The photo current density-voltage (J-S) curve of dye-sensitized solar cell based on (A) Ru-1 sensitizer, (B) Ru-2 sensitizer and C Ru-3 sensitizer.

The same illumination condition for Ru-3 sensitized solar cell gives J_{SC} 3.478, V_{OC} 6.3, FF 0.49 and that corresponds to an overall conversion efficiency of 1.05 %. The higher photo current density in these cell gave higher overall conversion efficiency, in the case of Ru-3 it has higher Jsc 3.489 than other two 2.79 and 0.78 for Ru-2 and Ru-1 respectively. This could be due to simple structure (Ru_{t2g}-π*orbital) of Ru-3 after photo excitation there is fast charge separation and injection of electron to the conduction band of TiO_2 semiconductor than the other two ruthenium sensitized solar cell. This could be ascribed to the electrons in the Highest Occupied Molecular Orbital (HOMO) Ru_{t2g} to the Lowest Unoccupied Molecular Orbital (LUMO).

Table 1. Absorption, emission of ruthenium complexes and J-V characteristic of dye sensitized solar cell fabricated using different ruthenium complexes Ru-1, Ru-2 and Ru-3 with total active area 0.6 cm^{-2} and input intensity light of 100mWcm^{-2}.

Cell Sensitizer	λ_{abs} (nm) & [MLCT(Ru t_2g-π*)	λ_{exc} (nm)	J_{SC}(mAcm^{-2})	V_{oc} (V)	FF	η (%)
Ru-1	305 and 533	700(18)	0.78	0.53	0.51	0.211
Ru-2	366 and 531	702(449)	2.79	0.593	0.498	0.82
Ru-3	310 and 523	690(14)	3.478	0.63	0.49	1.06

Thus the π*- ligand orbital undergo delocalization into more π-empty orbitals of phenanthroline than in bipyridine based ligand before injected into conduction band of the TiO_2 semiconductor.

However the poor overall conversion efficiency of all of these complexes might probably be due to leakage of electrolyte in the fabrication processes which lowers the photo current, open circuit voltage and overall conversion efficiencies. The volatile liquid electrolyte may inhibit the performance of the fabricated dye-sensitized solar cells.

4. CONCLUSIONS

Ruthenium(II) complexes of bipyridine and phenenthroline functionalized with –COOH, -SO_3H and COH were successfully synthesized, characterized and used for solar cells fabrication. The metal-to-ligand charge transfer (MLCT) transitions for these complexes appeared as prominent in the visible region in the range 510-533 nm of electromagnetic spectrum, and they have ability for photo sensitization. The photovoltaic performance of these Ru(II) complexes in the fabricated solar cells exhibited an overall solar light to electricity conversion efficiency of 1.06 greater than 0.84, and 0.21 % under artificial 1sun, global air mass AM 1.5 (100 $mWcm^{-2}$) illumination. The photo current density and overall efficiency mainly related with sunlight absorption ability of the dyes. The poor conversion efficiencies might be attributed to is due to lack of absorption by the compounds in the near IR region and also challenge of hole transporting material, that is leakage, and volatile liquid electrolytes. Thus this gives an idea about incorporating more π-conjugated substituents on both 2,9 and 4,7 positions of 1,10-phenanthroline to increase molar extinction coefficient which could improve light harvesting behaviour, open circuit voltage and the overall conversion efficiency.

ACKNOWLEDGEMENTS
The authors acknowledged with thanks the financial support of Govan Mbeki Research and Development Centre, University of Fort Hare Alice, CSIR, Pretoria South Africa for solar cell characterization and ACM thank Sasol Inzalo foundation-NRF for postgraduate scholarship.

References

1. A. J. Nozik, *Physica E,* 14 (2002) 115–120.
2. E. Stathatos, *J Engineering Sci Technol Rev.* 5 *(*2012) 9–13.
3. M. K. Nazeeruddin, P. Pechy, T. Renouard, S. M. Zakeeruddin, R. Humphry-baker, P. Comte, P. Liska, L. Cevey, E. Costa, V. Shklover, L. Spiccia, G. B. Deacon and C. A. Bignozzi, *J. Chem. Soc,* 123 *(*2001) 1613–1624.
4. A.O. Adeloye, T. O. Olomola, A. I. Adebayo and P. A. Ajibade, *Int, J. Mol. Sci,* 13 *(*2012) 3511–3526.
5. A.O. Adeloye, P. A. Ajibade, F. R. Cummings, L. J. Roux, S. N. Mamphweli and E.L. Meyer, *J. Chem. Sci,* 125 (2013) 17–27.
6. Y. Sun, S. N. Collins, L. E. Joyce, and C. Turro, *Inorg. Chem* 49 (2010) 4257–62.
7. M. Grätzel, *Purre Appl. Chem, 173 (*2001) 459–467.
8. M. K. Nazeeruddin, E. Baranoff and M. Grätzel, *Sol. Energy,* 85 (2011) 1172–1178.
9. J. Moser, M. Gratzel, J. Am. Chem. Soc, 106 (1984) 6557-6564.
10. M. Grätzel, *J. Photochem. Photobiol. C Photochem. Rev,* 4 *(*2003) 145–153.

11. L. Francis, A. S. Nair, R. Jose, S. Ramakrishna, V. Thavasi and E. Marsano, *Energy*, 36 (2011) 627–632.
12. O. Schwarz, D. Van Loyen, S. Jockusch, N. J. Turro and H. J. Dürr, *Photochem. Photobiol. A Chem*, 132 *(*2000) 91–98.
13. 28. Alessio, E. *Rev*, 104 *(*2004) 4203–4242.
14. I. P. Evans, A. Spencer and G. Wilkinson, *J. Chem. Soc. Dalt. Trans, (*1973) 204-209.
15. A. Harvey, M. Draganjac, S. Chui, R. Snell and E. Benjamin, *J. Arkansas Acad. Sci, 63 (*2009) 185.
16. C. A. Mitsopoulou, I. Veroni, I. A. Philippopoulos and P. Falaras, *J. Photochem. Photobiol. A Chem*, 191 *(*2007) 6–12.
17. Erten-ela, S. *Int. J. Photoenergy*, 2014 (2014) 1–6.
18. W. Zhao, H. Bala, J. Chen, Y. Zhao, G. Sun, J. Cao and Z. Zhang, *Electrochim. Acta*, 114 (2013) 318–324.
19. Y. Numata, S. P. Singh, A. Islam, M. Iwamura, A. Imai, K. Nozaki and L. Han, *Adv. Funct. Mater*, 23 (2013) 1817–1823.
20. T. Taziwa, E. Meyer, *Adv. Nanoparticle*, 3 (2014) 54–63.
21. E. Fourest and B. Volesky, *Enviro. Sci. Technol*, 30 (1996) 277–282.
22. K. Ocakoglu, E. Harputlu, P. Guloglu, and S. Erten-Ela, *Synth. Met*, 162 (2012) 2125–2133.
23. S. Verma, P. Kar, A. Das and N. H. Ghosh, *Dalton. Trans*, 40 (2011) 9765–731.
24. L. Giribabu, V.K. Singh, C. V. Kumar, Y. Soujanya, V. G. Reddy and P. Y. Reddy, *Adv. Optoelectron*, 2011 *(*2011) 1–8
25. K. Takagi, S. Magaino, H. Saito, T. Aoki, and D. Aoki, *J. Photochem. Photobiol. C Photochem. Rev*, 14 (2013) 1–12.